Resonant reflection of interacting electrons from an impurity in a quantum wire: Interplay of Zeeman and spin-orbit effects

Rajesh K. Malla and M. E. Raikh
Department of Physics and Astronomy, University of Utah, Salt Lake City, Utah 84112, USA

(Received 5 August 2018; published 9 October 2018)

A single-channel quantum wire with two well-separated Zeeman subbands and in the presence of weak spin-orbit coupling is considered. An impurity level which is split off the upper subband is degenerate with the continuum of the lower subband. We show that, when the Fermi level lies in the vicinity of the impurity level, the transport is completely blocked. This is the manifestation of the effect of resonant reflection and can be viewed as resonant tunneling between left-moving and right-moving electrons via the impurity level. We incorporate electron-electron interactions and study their effect on the shape of the resonant-reflection profile. This profile becomes a two-peak structure, where one peak is caused by resonant reflection itself, while the origin of the other peak is reflection from the Friedel oscillations of the electron density surrounding the impurity.

DOI: 10.1103/PhysRevB.98.144202

I. INTRODUCTION

Electron states in a ballistic wire in the presence of spin-orbit coupling became the subject of intensive theoretical (see, e.g., Refs. [1–7]) and experimental [8–11] studies almost three decades ago. The initial motivation for these studies was the proposal of a spin transistor by Das and Datta [12]. The motivation for the later studies was the proposal [13,14] that, in the proximity of a superconductor, the interplay of spin-orbit coupling and Zeeman splitting can lead to the formation of zero-energy bound states at the wire ends. Yet another motivation for the research on the combined action of Zeeman and spin-orbit fields comes from the recent experiments on cold gases [15].

Nontriviality of the interplay of spin-orbit coupling and Zeeman splitting manifests itself already in the ballistic transport through the wire. It was predicted [1,2] and confirmed experimentally [8] that, as a result of this interplay, the dependence of the conductance on the Fermi level can become nonmonotonic. Such a "spin gap" develops when the spin-orbit minimum in the energy spectrum of a free electron is comparable to the Zeeman splitting. Another nontrivial consequence of the interplay shows up when the spin-orbit coupling is inhomogeneous [3–7]. Namely, a steplike inhomogeneity can lead to a full reflection of the incident electron.

The underlying physics of the full reflection is the same as the physics of the resonant reflection in the two-subband wire first studied in Refs. [16,17]. It does not require either Zeeman field or spin-orbit coupling. An attractive impurity in a two-subband wire splits off an energy level from the bottom of both subbands. If the Fermi level, lying in the lower subband, coincides with the level split from the upper subband (see Fig. 1), the transport involves multiple virtual visits to this level. As it was first shown in Ref. [16], the outcome of these visits is a reflection rather than resonant transmission as one would naively expect. In a single-channel wire the role of the size-quantization subbands is played by the spin subbands, while the visits to the split-off level are enabled by the spin-orbit coupling.

The goal of the present paper is to study the effect of electron-electron interactions on the resonant reflection. For a single-channel interacting wire it is accepted that any weak potential impurity blocks completely the zero-temperature transport through the wire. The theories [18] which capture this phenomenon are the Luttinger-liquid description and backscattering by the Friedel oscillations in an electron gas imposed by an impurity. In the latter case, the role of the interactions is simply a conversion of the oscillations of electron density into the oscillations of the potential. As first pointed out in Refs. [19,20] (see also later papers [21,22]), the period of the Friedel oscillations matches the Bragg condition for an electron at the Fermi level. Thus, the electron is scattered by a compound object consisting of the impurity itself and the oscillating potential, which it creates.

The theory of Refs. [19,20] was later generalized to the case of a pair of impurities [23,24]. The specific of the pair is that an electron can bounce between the constituting impurities for a long time. As a result of this bouncing, a quasilocal level degenerate with the continuum is formed. For an incident electron with energy in resonance with this quasilocal level the transmission coefficient is close to 1. Physically, the results of Refs. [23,24] can be interpreted as follows. When the incident electron is resonantly transmitted, the Friedel oscillations do not form, so that the interactions suppress the transmission only when the Fermi level is spaced away from the resonant level.

Contrary to the resonant transmission, in the case of the resonant reflection the Friedel oscillations are the strongest when the Fermi level lies close to the impurity level. Thus, the modification of the resonant reflection profile due to interactions is also strong. This demands a more detailed treatment of the partial reflection of an electron on the way to the impurity than the renormalization-group scheme adopted

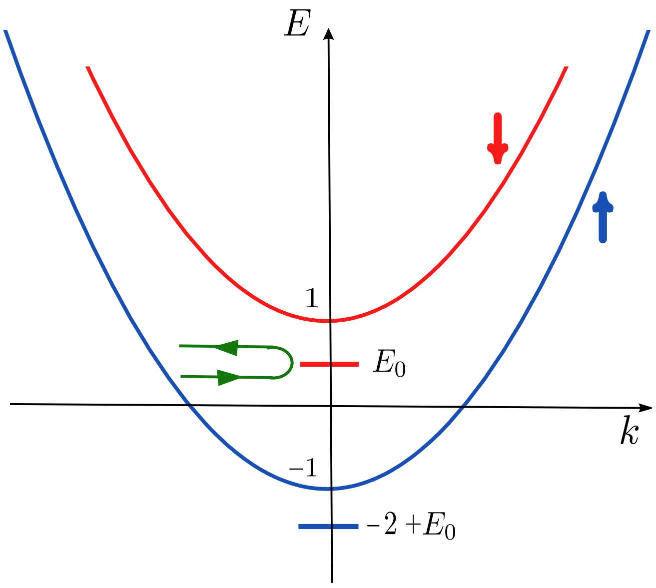

FIG. 1. Schematic illustration of the resonant reflection. An attractive impurity creates bound states under the bottoms of ↓ (red) and ↑ (blue) subbands. The binding energy, measured in units of Δ, is $1-E_0$. Weak spin-orbit coupling mixes ↓ and ↑ wave functions. As a result, an incident ↑ electron undergoes a resonant scattering, illustrated by the green line. The result of the scattering is almost full reflection rather than conventional resonant transmission.

in Refs. [19–24]. Our most spectacular finding is that, for certain phases accumulated by the electron on the way to the impurity, the resonant reflection from the bare impurity can turn into the resonant transmission.

II. RESONANT REFLECTION

In the presence of the Zeeman field and spin-orbit coupling, the Hamiltonian of a wire has the form

$$\hat{H} = \begin{pmatrix} -\frac{\hbar^2 k_x^2}{2m} - \Delta & i\gamma k_x \\ -i\gamma k_x & -\frac{\hbar^2 k_x^2}{2m} + \Delta \end{pmatrix}, \tag{1}$$

where m is the electron mass, 2Δ is the Zeeman splitting, and γ is the spin-orbit coupling strength (for concreteness we have chosen the spin-orbit Hamiltonian to be of the Rashba type).

We assume that the impurity potential is short ranged, $V(x) = V_0\delta(x)$. The system of coupled equations for ↑ and ↓ components of the spinor reads

$$-\frac{\hbar^2}{2m}\frac{\partial^2\psi_1}{\partial x^2} + V_0\delta(x)\psi_1 - (\varepsilon+\Delta)\psi_1 = \gamma\frac{\partial\psi_2}{\partial x},$$
$$-\frac{\hbar^2}{2m}\frac{\partial^2\psi_2}{\partial x^2} + V_0\delta(x)\psi_2 - (\varepsilon-\Delta)\psi_2 = -\gamma\frac{\partial\psi_1}{\partial x}. \tag{2}$$

Since the energy of the incident ↑ electron in resonance with the impurity level of the ↓ electron is close to Δ (see Fig. 1), it is convenient to introduce the following dimensionless variables:

$$z = \frac{x}{x_0}, \quad E = \frac{\varepsilon}{\Delta},$$
$$\alpha = \left(\frac{2mx_0}{\hbar^2}\right)\gamma, \quad U_0 = \left(\frac{2mx_0}{\hbar^2}\right)V_0, \tag{3}$$

where the characteristic length,

$$x_0 = \left(\frac{\hbar^2}{2m\Delta}\right)^{1/2}, \tag{4}$$

is the de Broglie wavelength of the electron with energy $\varepsilon = \Delta$. In the dimensionless variables the system (2) takes the form

$$-\frac{\partial^2\psi_1}{\partial z^2} + U_0\delta(z)\psi_1 - (E+1)\psi_1 = \alpha\frac{\partial\psi_2}{\partial z},$$
$$-\frac{\partial^2\psi_2}{\partial z^2} + U_0\delta(z)\psi_2 - (E-1)\psi_2 = -\alpha\frac{\partial\psi_1}{\partial z}. \tag{5}$$

Without impurity, the solutions of the system (5) in the domain $-1 < E < 1$ correspond to propagation of the ↑ spin component and the decay of the ↓ spin component (see Fig. 1). Due to spin-orbit coupling, both components of the corresponding spinors are nonzero,

$$\begin{pmatrix}\psi_1\\ \psi_2\end{pmatrix} = \begin{pmatrix}1\\ iC\end{pmatrix}e^{iqz}, \quad \begin{pmatrix}\psi_1\\ \psi_2\end{pmatrix} = \begin{pmatrix}D\\ 1\end{pmatrix}e^{-\kappa z}, \tag{6}$$

where the wave vector q, the decay constant κ, and the components C and D of the spinors are given by

$$q(E) = (1+E)^{1/2}, \quad \kappa(E) = (1-E)^{1/2},$$
$$C = \frac{1}{2}\alpha q, \quad D = \frac{1}{2}\alpha\kappa. \tag{7}$$

Coefficients C and D describe the admixture of the opposite spin projection due to spin-orbit coupling.

In the presence of impurity, the general solution at $z < 0$ has the form

$$\begin{pmatrix}\psi_1\\ \psi_2\end{pmatrix} = \begin{pmatrix}1\\ iC\end{pmatrix}e^{iqz} + r_1\begin{pmatrix}1\\ -iC\end{pmatrix}e^{-iqz} + r_2\begin{pmatrix}D\\ 1\end{pmatrix}e^{\kappa z}, \tag{8}$$

which is the combination of the solutions (6). The first two terms describe the incident and reflected ↑ waves, while the third term describes the solution corresponding to ↓, which decays at $z \to -\infty$.

The corresponding solution for $z > 0$ reads

$$\begin{pmatrix}\psi_1\\ \psi_2\end{pmatrix} = t_1\begin{pmatrix}1\\ iC\end{pmatrix}e^{iqz} + t_2\begin{pmatrix}-D\\ 1\end{pmatrix}e^{-\kappa z}. \tag{9}$$

The first term describes the transmitted ↑ wave, while the second term describes the decay of the ↓ component.

Although the parameters C and D are proportional to α and thus are small due to the weakness of the spin-orbit coupling, it is these admixtures that are responsible for the resonant reflection. To capture this effect, we follow the standard procedure and calculate the reflection and transmission coefficients from the system of boundary conditions at $z = 0$.

Continuity of the wave function equations (8) and (9) yields two conditions,

$$\begin{aligned} 1 + r_1 + r_2 D &= t_1 - t_2 D, \\ iC(1 - r_1) + r_2 &= iCt_1 + t_2. \end{aligned} \tag{10}$$

The other two conditions come from the discontinuity of the derivatives, $\frac{\partial \psi_1}{\partial z}$ and $\frac{\partial \psi_2}{\partial z}$, at $z = 0$. Integrating the system (5) near $z = 0$, we get

$$\begin{aligned} iqt_1 + \kappa t_2 D - [iq(1 - r_1) + \kappa r_2 D] &= U_0(t_1 - t_2 D), \\ -qCt_1 - \kappa t_2 - [-qC - qCr_1 + \kappa r_2] &= U_0(iCt_1 + t_2). \end{aligned} \tag{11}$$

Simplifying the above boundary conditions by introducing $R_2 = Dr_2$, $T_2 = Dt_2$, and $\lambda = CD$, we get

$$\begin{aligned} R_2 + T_2 &= t_1 - r_1 - 1, \\ R_2 - T_2 &= i\lambda(t_1 + r_1 - 1), \end{aligned} \tag{12}$$

$$\begin{aligned} iq(t_1 + r_1) - U_0 t_1 - iq &= R_2\kappa - (\kappa + U_0)T_2, \\ (\kappa + U_0)T_2 + \kappa R_2 &= -\lambda[-it_1(iq - U_0) - q(1 + r_1)]. \end{aligned} \tag{13}$$

Since we are interested in the reflection and transmission coefficients, r_1 and t_1, it is convenient to express R_2 and T_2 from the system (12) and substitute them into the system (13), which assumes the form

$$t_1 + r_1 = \frac{\left[q - \lambda\left(\kappa + \frac{U_0}{2}\right)\right] + i\frac{U_0}{2}}{\left[q - \lambda\left(\kappa + \frac{U_0}{2}\right)\right] - i\frac{U_0}{2}}, \tag{14}$$

$$t_1 - r_1 = \frac{\kappa + \frac{U_0}{2} + q\lambda - i\lambda\frac{U_0}{2}}{\kappa + \frac{U_0}{2} + q\lambda + i\lambda\frac{U_0}{2}}. \tag{15}$$

We see that the absolute values of $t_1 + r_1$ and $t_1 - r_1$ are equal to 1. Then it is convenient to cast the solution of the system (14) into the form

$$|r_1|^2 = \sin^2(\Phi_- - \Phi_+), \quad |t_1|^2 = \cos^2(\Phi_- - \Phi_+), \tag{16}$$

where

$$\begin{aligned} \Phi_+ &= \frac{1}{2}\tan^{-1}\frac{\frac{U_0}{2}}{q - \lambda(\kappa + \frac{U_0}{2})}, \\ \Phi_- &= \frac{1}{2}\tan^{-1}\frac{\frac{\lambda U_0}{2}}{\kappa + \frac{U_0}{2} + q\lambda}. \end{aligned} \tag{17}$$

Until now the calculation was exact. The weakness of the spin-orbit coupling, quantified by the condition $\alpha \ll 1$, was used in the explicit expressions for q and κ. We will now use this condition to simplify the phases Φ_+ and Φ_-. First, we note that the dimensionless parameter

$$\lambda = CD = \frac{1}{4}\alpha^2(1 - E^2)^{1/2} \tag{18}$$

is quadratic in spin-orbit coupling strength. This allows us to simplify Φ_+ to $\tan^{-1}(\frac{U_0}{2q})$. Then Φ_+ can be identified with the scattering phase of the $\uparrow$ electron from the impurity *in the absence of spin-orbit coupling*.

Turning to the phase Φ_-, we note that the small parameter α^2 in the expression for λ allows us to neglect the term $q\lambda$ in the denominator. Then we see that, for attractive impurity, $U_0 < 0$, this denominator becomes zero at energy $E = E_0$, determined by the condition

$$\kappa(E_0) = \frac{|U_0|}{2}. \tag{19}$$

This condition expresses the fact that *in the absence of spin-orbit coupling*, the energy position of the level of the $\downarrow$ electron in the potential $U_0\delta(z)$ is $E = E_0$ (see Fig. 1).

To establish the energy width Γ of the resonance, we recast the expression for $\tan\Phi_-$ into the form

$$\tan[\Phi_-(E)] = \frac{1}{8}\alpha^2(1 - E^2)^{1/2}|U_0|\left[\frac{(1 - E^2)^{1/2} + \frac{|U_0|}{2}}{1 - E - \frac{U_0^2}{4}}\right]. \tag{20}$$

Near the resonance, $E = E_0 = 1 - \frac{U_0^2}{4}$, expression (20) assumes the conventional Breit-Wigner form

$$\tan[\Phi_-(E)] = \frac{\Gamma}{E_0 - E}, \tag{21}$$

where Γ is given by

$$\Gamma = \frac{\alpha^2}{16}|U_0|^3. \tag{22}$$

With the binding energy of the $\downarrow$ electron being $\frac{U_0^2}{4}$, we see that the width Γ is much smaller than this binding energy, which justifies the expansion near the resonance.

If the bound state in the potential $U_0\delta(z)$ is shallow, i.e., $U_0 \ll 1$, we can replace $\tan^{-1}$ in the expression for Φ_+ by the argument. After that, the final expression for the energy-dependent reflection coefficient assumes the form

$$\begin{aligned} |r_1(E)|^2 &= \sin^2\left[\tan^{-1}\left(\frac{\Gamma}{E_0 - E}\right) - \frac{|U_0|}{2q}\right] \\ &= \frac{\left[\Gamma - \frac{|U_0|}{2q}(E_0 - E)\right]^2}{(E_0 - E)^2 + \Gamma^2}. \end{aligned} \tag{23}$$

It follows from Eq. (23) that $|r_1(E)|^2$ has a characteristic Fano shape [25]. Near the resonance, $E = E_0$, it is a Lorentzian with the width Γ. As the energy is swept through E_0, the reflection coefficient passes through zero (antiresonace) before returning to its nonresonant value $|r_1|^2 = \frac{|U_0|^2}{4q^2}$.

III. INCORPORATING THE ELECTRON-ELECTRON INTERACTIONS

As explained in the Introduction, the effect of interactions is more pronounced in the case of resonant reflection than in the case of resonant transmission [23,24]. The reason is that the amplitude of the Friedel oscillations is proportional to the reflection amplitude [19,20], which, for resonant reflection, is close to 1. On the other hand, the Friedel oscillation of electron density creates perturbations which play the role of the "Bragg mirrors" for incident and transmitted electron waves. As a result of Friedel oscillations being strong, each Bragg mirror is highly "reflective." This suggests incorporating the

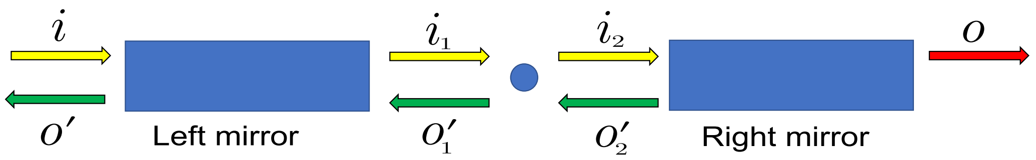

FIG. 2. Schematic illustration of the electron scattering from impurity "dressed" by Friedel oscillations, which play the role of the Bragg mirrors. The incident electron i can be reflected by the left mirror, by the impurity, or by the right mirror.

effect of attenuation, caused by the mirrors, more accurately than in Refs. [23,24].

The process of electron reflection from a compound object consisting of three scatterers, two Bragg mirrors, and an impurity between them is illustrated in Fig. 2. The rigorous way to describe this reflection analytically is to employ the scattering matrices of each scatterer relating the amplitudes of the incoming and outgoing partial waves. These matrices are defined as follows:

$$\begin{pmatrix} i_1 \\ o' \end{pmatrix} = \begin{pmatrix} t_L & r_L \\ -r_L^* & t_L^* \end{pmatrix}\begin{pmatrix} i \\ o_1' \end{pmatrix}, \quad \begin{pmatrix} i_2 \\ o_1' \end{pmatrix} = \begin{pmatrix} t_1 & r_1 \\ -r_1^* & t_1^* \end{pmatrix}\begin{pmatrix} i_1 \\ o_2' \end{pmatrix}, \quad \begin{pmatrix} o \\ o_2' \end{pmatrix} = \begin{pmatrix} t_R & r_R \\ -r_R^* & t_R^* \end{pmatrix}\begin{pmatrix} i_2 \\ 0 \end{pmatrix}. \tag{24}$$

The amplitude r_1 in Eq. (24) was found in the previous section. The two remaining amplitudes, r_L and r_R, will be calculated later. Excluding the intermediate amplitudes i_1, i_2, o_1', o_2' from Eq. (24), we find the expression for the net amplitude reflection coefficient of the compound scatterer

$$r_{\text{eff}} = -\frac{o'}{i} = \frac{r_L^* + r_1^* + r_R^* + r_L^* r_1 r_R^*}{1 + r_1 r_R^* + r_L r_1^* + r_L r_R^*}. \tag{25}$$

To analyze this expression, we express the reflection coefficient $|r_{\text{eff}}|^2$ via the magnitudes of the reflection coefficients r_1, r_L, and r_R and obtain

$$|r_{\text{eff}}|^2 = 1 - |t_{\text{eff}}|^2 = 1 - \frac{(1-|r_{\text{Bragg}}|^2)^2(1-|r_1|^2)}{(1+|r_{\text{Bragg}}|^2 + 2|r_{\text{Bragg}}||r_1|\cos\beta)^2}. \tag{26}$$

In Eq. (26) we took into account that, unlike in Refs. [23,24], there is symmetry between the left and right mirrors, so that the magnitudes $|r_L|$ and $|r_R|$ are equal to each other and are denoted by $|r_{\text{Bragg}}|$. The phase β is the combination of the phase Φ_-, defined by Eq. (16), and the phase Φ_{Bragg}, accumulated in the course of the reflection from the mirror. We will see that this phase is big and depends strongly on the energy. Thus, we average Eq. (26) over β using the identity

$$\left\langle \frac{1}{(a+\cos\beta)^2} \right\rangle_\beta = \frac{a}{(a^2-1)^{3/2}}. \tag{27}$$

The result of this averaging reads

$$\langle |r_{\text{eff}}|^2 \rangle = 1 - \frac{(1-|r_{\text{Bragg}}|^2)^2(1+|r_{\text{Bragg}}|^2)(1-|r_1|^2)}{[(1-|r_{\text{Bragg}}|^2)^2 + 4|r_{\text{Bragg}}|^2(1-|r_1|^2)]^{3/2}}. \tag{28}$$

It is also instructive to express the effective transmission coefficient via the partial transmission coefficients $|t_1|^2$ and $|t_{\text{Bragg}}|^2$. One obtains

$$\langle |t_{\text{eff}}|^2 \rangle = \frac{|t_{\text{Bragg}}|^4 (2-|t_{\text{Bragg}}|^2)|t_1|^2}{[|t_{\text{Bragg}}|^4 + 4(1-|t_{\text{Bragg}}|^2)|t_1|^2]^{3/2}}. \tag{29}$$

Since the transmission $|t_{\text{Bragg}}|^2$ is strongly dependent on the position of the Fermi level E_F with respect to the resonant energy level E_0, the magnitude of $|t_{\text{Bragg}}|^2$ falls off with increasing $(E_F - E_0)$. Then one would expect $|t_{\text{eff}}|^2$ to grow monotonically with increasing $|t_{\text{Bragg}}|^2$ and to approach $|t_1|^2$. The reasoning behind this expectation is that the scattering by the Bragg mirrors becomes inefficient for large $(E_F - E_0)$. Remarkably, the dependence of $|t_{\text{eff}}|^2$, described by Eq. (29), is *nonmonotonic*. As illustrated in Fig. 3, this dependence has a maximum. For small transmission of the impurity, $|t_1|^2 \ll 1$, the position of the maximum is easy to calculate analytically. It is $|t_{\text{Bragg}}|^4 = 8t_1^2$. Note that the value $|t_{\text{Bragg}}|^4$ has a meaning of the net transmission of *two mirrors*. Thus, the maximum occurs when the transmissions of the impurity and of the two mirrors are equal within a numerical factor. Substituting $|t_{\text{Bragg}}|^4 = 8t_1^2$ into Eq. (29), we find the maximal value of the effective transmission

$$(|t_{\text{eff}}|^2)_{\text{max}} = \frac{2}{3^{3/2}}|t_1|. \tag{30}$$

We see that this value is *much bigger* than $|t_1|^2$.

The origin of the maximum is that the dominant contribution to the phase-averaged transmission $\langle |t_{\text{eff}}|^2 \rangle$ comes from the phases β in Eq. (26) for which the denominator is close to zero. In other words, while the impurity alone acts

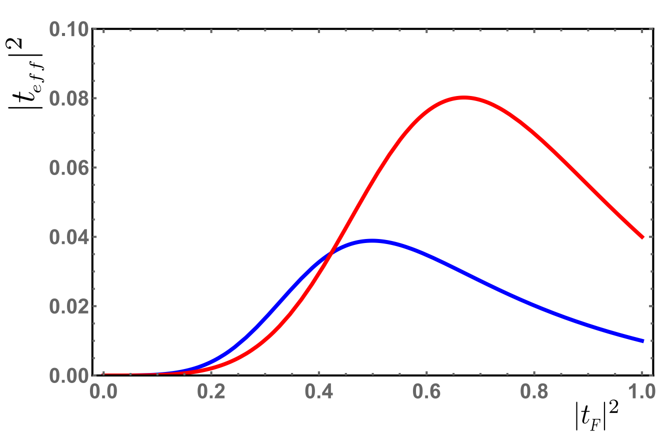

FIG. 3. Effective transmission coefficient of the impurity dressed by the Friedel oscillations is plotted from Eq. (29) versus the transmission of the Bragg mirrors for $|t_1|^2 = 0.01$ (blue) and $|t_1|^2 = 0.04$ (red).

as a reflector, adding the two Bragg mirrors can lead to the *resonant transmission*.

Naturally, the values of $|t_1|^2$ and $|t_{\rm Bragg}|^2$ are not independent. It is the reflection from the impurity that controls the magnitude of the Friedel oscillations. To analyze the behavior of the effective transmission with energy E of the incident electron and with E_F, we need to specify the analytical form of $|t_{\rm Bragg}|^2$. This is done in the next section.

IV. TRANSMISSION OF THE BRAGG MIRROR

In the presence of electron-electron interactions, propagation of an electron through the mirror is described by the Schrödinger equation

$$-\frac{\partial^2\psi_1}{\partial z^2}+V_H(z)\psi_1+\hat{V}_{ex}\{\psi_1\}=(E+1)\psi_1, \tag{31}$$

where $V_H(z)$ and $\hat{V}_{ex}$ are the Hartree and exchange terms, respectively. When the interaction is short ranged, one can consider only the Hartree term since the exchange term causes only a modification of the interaction constant [19]. The other consequence of the interaction being short ranged is that the Hartree potential is proportional to the modulation of the electron density created by the Friedel oscillations [19]; that is, it has the from

$$V_H(z)=\frac{\mu(E_F)}{q_F|z|}\cos(2q_F|z|), \tag{32}$$

where q_F is the Fermi momentum. The magnitude of the electron-electron interactions and the energy dependence of $|r_1|$, which is responsible for the Friedel oscillations, are encoded into the constant μ, which we will specify later. The main difference between our approach and the approach of Ref. [19] is that we find an asymptotically exact solution of Eq. (31), while in Ref. [19] it was solved perturbatively. The reason the asymptotically exact solution can be found is that the amplitude of $V_H(z)$ falls off slowly with z, so that the relevant values of q_Fz are big. This, in turn, suggests searching for $\psi_1(z)$ in the form

$$\psi_1(z)=A_+(z)e^{iq_Fz}+A_-(z)e^{-iq_Fz}, \tag{33}$$

where the functions A_+ and A_- change slowly with z, so that their second derivatives can be neglected. Upon substituting Eq. (33) into Eq. (31) and neglecting nonresonant terms $\exp(\pm 3iq_Fz)$, we arrive at a coupled system of the first-order equations

$$\begin{aligned}-2iq_F\frac{\partial A_+(z)}{\partial z}+\frac{\mu}{2z}A_-(z)&=\big(E+1-q_F^2\big)A_+(z),\\ 2iq_F\frac{\partial A_-(z)}{\partial z}+\frac{\mu}{2z}A_+(z)&=\big(E+1-q_F^2\big)A_-(z).\end{aligned} \tag{34}$$

It appears that this system can be solved *exactly* for arbitrary interaction strength μ. To see this, we first perform a rescaling,

$$y=z\left(\frac{E+1-q_F^2}{2q_F}\right), \tag{35}$$

and then introduce the auxiliary functions

$$a(y)=A_+(y)+iA_-(y),\ b(y)=A_+(y)-iA_-(y). \tag{36}$$

Then the system (34) reduces to

$$\begin{aligned}\frac{\partial a}{\partial y}+\frac{\mu}{4q_Fy}a(y)&=ib(y),\\ \frac{\partial b}{\partial y}-\frac{\mu}{4q_Fy}b(y)&=ia(y).\end{aligned} \tag{37}$$

In the rescaled form, the system contains a single dimensionless parameter, $\frac{\mu}{4q_F}$. As a next step, we substitute $b(y)$ from the first equation into the second equation and arrive at the following second-order differential equation:

$$\frac{\partial^2 a}{\partial y^2}+\left[1+\frac{1-4(\frac{\mu}{4q_F}+\frac{1}{2})^2}{4y^2}\right]a(y)=0. \tag{38}$$

The general solution of this equation can be presented as a linear combination,

$$a(y)=y^{1/2}\Big[c_1J_{\frac{\mu}{4q_F}+\frac{1}{2}}(y)+c_2J_{-\frac{\mu}{4q_F}-\frac{1}{2}}(y)\Big], \tag{39}$$

where $J_{\frac{\mu}{4q_F}+\frac{1}{2}}$ and $J_{-\frac{\mu}{4q_F}-\frac{1}{2}}$ are the Bessel functions. At large y both Bessel functions oscillate, so that the value of the transmission coefficient is governed by the ratio c_1/c_2. This ratio is determined by the condition that at small $y=y_c$, where the Friedel oscillations are terminated (see Appendix A), the amplitude of the reflected wave vanishes. The final expression for the transmission coefficient reads

$$t_{\rm Bragg}=\frac{(2\pi y_c)^{1/2}J_{\frac{\mu}{4q_F}-\frac{1}{2}}(y_c)J_{-\frac{\mu}{4q_F}-\frac{1}{2}}(y_c)}{J_{\frac{\mu}{4q_F}-\frac{1}{2}}(y_c)e^{i\frac{\pi\mu}{8q_F}}+J_{-\frac{\mu}{4q_F}-\frac{1}{2}}(y_c)e^{-i\frac{\pi\mu}{8q_F}}}. \tag{40}$$

The details of the derivation are presented in Appendix B.

The result (40) can be simplified when y_c is small. Then we can use the small-argument asymptotes of the Bessel functions and obtain

$$t_{\rm Bragg}=\frac{1}{\cosh\left(\frac{\mu}{4q_F}\ln y_c\right)}. \tag{41}$$

In deriving this expression we took into account that the interactions are weak in the usual sense, namely, that the typical interaction energy is much smaller than the Fermi energy. This condition ensures that $\frac{\mu}{q_F}$ is small.

Concerning the value of y_c, in Appendix A it is demonstrated that the Friedel oscillations are terminated at $z=z_c\sim\frac{q_0}{\Gamma}$. Using the relation (35), we find that, within a numerical factor, y_c is given by

$$y_c=\frac{E-E_F}{\Gamma}. \tag{42}$$

We see that in the interesting limit when the Fermi level is close to the resonance, y_c is indeed small.

Equations (41) and (42) describe how the transmission of the Bragg mirror evolves with energy. Indeed, the argument of the hyperbolic cosine is the product of a small factor $\frac{\mu}{4q_F}$ and a big factor $\ln y_c$. If this product is small, e.g., when the interactions are weak, then the transmission coefficient is close to 1. On the contrary, if the product is big, we have

$$t_{\rm Bragg}=\left(\frac{2|E-E_F|}{\Gamma}\right)^{\frac{|\mu|}{4q_F}}\ll 1; \tag{43}$$

that is, the mirror is highly reflective.

To conclude this section, we present the microscopic expression for the parameter μ in terms of the Fourier components of the interaction potential. This expression follows from the expression for the amplitude of the oscillations of the electron density, calculated in Appendix A, and has the form

$$\mu = \frac{\nu q_F}{2}|r_1(E_F)|^2, \tag{44}$$

where ν is given by

$$\nu = \frac{V(0) - V(2q_F)}{2\pi\hbar v_F}. \tag{45}$$

The term $V(0)$ comes from the exchange potential, while $V(2q_F)$ comes from the Hartree potential; v_F stands for the Fermi velocity.

Note that the transmission t_{Bragg} is full not only in the absence of electron-electron interactions. If the interactions are present but there is no reflection from the impurity, $r_1(E_F) = 0$, then transmission is also full. This is natural since, in the absence of reflection, the Friedel oscillations do not form.

V. ENERGY DEPENDENCE OF THE EFFECTIVE REFLECTION

In Eq. (29) both t_1 and t_{Bragg} are functions of energy. While t_1 is a growing function of energy, t_{Bragg} grows with increasing $|E - E_F|$. In addition, the power $\frac{\mu}{4q_F}$ in Eq. (43) depends on the difference $|E_0 - E_F|$ (see Appendix A).

Concerning the overall dependence $|r_{\text{eff}}(E)|^2$, the situation is most transparent when the Fermi level lies away from the resonance. Then the presence of the Bragg mirrors manifests itself only near $E = E_F$. Bragg mirrors cause a spike in the reflection. When the spacing between E_F and E_0 is much smaller than the width of the resonance, there are two features in the $|r_{\text{eff}}(E)|^2$ dependence that are present for any interaction strength. First, the reflection is full for any position of the Fermi level when the energy of the incident electron is $E = E_0$. This is because the electron is fully reflected even in the absence of the Friedel oscillations. Second, $|r_{\text{eff}}(E)|^2 = 1$ at $E = E_F$ due to full reflection from the mirror. Thus, in the domain $-E_F < E < 0$, the reflection coefficient should pass through a minimum. Indeed, this minimum is present in the curves $|r_{\text{eff}}(E)|^2$ plotted from Eqs. (28) and (41) in Fig. 4.

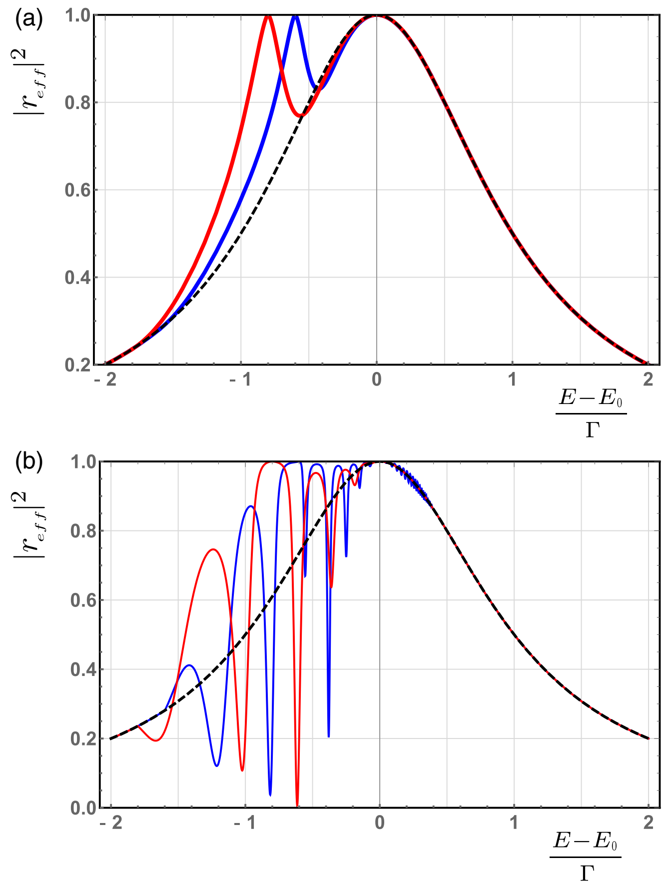

FIG. 4. (a) In the absence of interactions, the effective reflection coefficient is a Lorentzian, $|r_{\text{eff}}|^2 = [1 + \frac{(E-E_0)^2}{\Gamma^2}]^{-1}$ (black dashed line). With interactions, full reflection takes place at two energies, at $E = E_0$ as a result of scattering from the impurity and at $E = E_F$ as a result of scattering from the Bragg mirror. This is illustrated by red and blue curves plotted from Eqs. (28) and (41) for $(E_0 - E_F) = 0.8\Gamma$ and $(E_0 - E_F) = 0.6\Gamma$, respectively. The interaction strength in both curves is chosen to be $\frac{\mu}{4q_F} = 0.4$. (b) Scattering by two Bragg mirrors can, for certain energies, transform the resonant reflection into the resonant transmission. While (a) shows the average over the phase, β, (b) shows the reflection profile for the same parameters *prior to averaging*.

VI. DISCUSSION

(i) To establish the relation between our results and those obtained within the renormalization-group approach [19–24] we assume that the reflection of the Bragg mirrors is weak and expand Eq. (26) with respect to $|r_{\text{Bragg}}|^2$. This yields

$$|r_{\text{eff}}|^2 - |r_1|^2 = 4(1 - |r_1|^2)[|r_{\text{Bragg}}|^2 + |r_1||r_{\text{Bragg}}|\cos\beta]. \tag{46}$$

The second term in the brackets contains the first power of $|r_{\text{Bragg}}|$, unlike the first term, which contains $|r_{\text{Bragg}}|^2$. This second term comes from the interference of incident and reflected waves passing through the Bragg mirror. If we average Eq. (46) over β, the second term will disappear. Then it is the first term, $1 - t^2_{\text{Bragg}}$, that will describe the reduction of the transmission of the impurity due to electron-electron interactions. As follows from Eq. (41), $|r_{\text{Bragg}}|^2$ is proportional to $|r_1|^2$ and contains $\mu \ln y_c$. Then Eq. (46) reproduces the main result of Ref. [19]. In Ref. [19] this result is subsequently converted to the renormalization-group equation. We studied the limit in which both $|r_1|$ and $|r_{\text{Bragg}}|$ are close to 1. Then the denominator in Eq. (26) is close to zero when $\cos\beta = -1$. Definitely, the expansion with respect to $|r_{\text{Bragg}}|$ and the subsequent summation of the leading terms, which is the essence of the renormalization-group approach, do not capture this resonant transmission.

(ii) Adopting the renormalization-group approach in Refs. [19–24] relies on the assumption that the coefficients of the expansion of $|t_{\text{eff}}|^2$ in powers of $\ln(|E - E_F|)$ fall off as $\frac{1}{n!}$. Our calculation is equivalent to the summation of all the orders of the expansion and confirms this assumption.

(iii) The form (23) of the resonant reflection is the same as for the resonant tunneling between the two electrodes via a localized state located between the electrons. This suggests the interpretation of the resonant transmission as resonant tunneling *between left-moving and right-moving electrons*. If this interpretation is correct, the width Γ calculated from the golden rule should coincide with Eq. (22) and, in particular, should be proportional to U_0^3. Taking into account that the normalized wave function of the localized state has the form $\psi_2(z) = \kappa^{1/2}\exp(-\kappa|z|)$, the matrix element of $\alpha\frac{\partial}{\partial z}$ between $\psi_2(z)$ and the right-moving plane wave, $\exp(iqz)$, is given by

$$i\alpha\kappa^{1/2}q\int_{-\infty}^{\infty}dz\exp[iqz-\kappa|z|] = 2i\frac{q\kappa^{3/2}}{q^2+\kappa^2}. \tag{47}$$

One can neglect κ^2 in the denominator. Then the square of the matrix element is proportional to κ^3 and thus to U_0^3 since, at resonance, $\kappa = \frac{U_0}{2}$.

(iv) There is a question whether the attenuation of electron wave functions upon passage of the Bragg mirrors disturbs the shape of the Friedel oscillations. It is important that this disturbance is negligible. Qualitatively, this follows from the fact that many states with $E < E_F$ are responsible for the formation of the Bragg mirrors, while only the states with $|E - E_F| \lesssim \nu\Gamma$ are strongly affected by the Bragg mirrors.

(v) Another question is why we did not take into account the Friedel oscillations originating from the electron reflection within the same subband. Indeed, while the Friedel oscillations caused by the resonant reflection develop at large distances $z_c \sim \frac{q_0}{\Gamma}$, "nonresonant" Friedel oscillations start at much smaller $z \sim 1$. To answer this question one should estimate the contribution to the reflection coefficient within the domain $1 < z < z_c$, where nonresonant Friedel oscillations dominate. The amplitude of these oscillations is $\sim \frac{U_0}{q_F}$, and they fall off as $1/z$. This leads to the estimate $\frac{U_0}{q_F}\ln(z_c)$ as in Ref. [19]. Since $\frac{U_0}{q_F} \ll 1$, the weakness of nonresonant reflection cannot be compensated by the logarithmically big factor $\ln(\frac{q_0}{\Gamma})$; it is for this reason that we have neglected the Friedel oscillations originating from the reflection within the same subband.

On physical grounds, the electron incident from $z \to -\infty$ encounters the "resonant" Friedel oscillation first, and then, as $|z|$ becomes smaller than z_c, it passes through the "nonresonant" Friedel oscillation and experiences the additional reflection. Then the criterion $\frac{U_0}{2q_F}\ln(z_c) \ll 1$ ensures that the resonant reflection with amplitude close to 1 is much stronger than nonresonant reflection.

Formally, both processes, the reflections from resonant and from nonresonant Friedel oscillations, are described by the system (34). For resonant reflection, the value of μ is given by Eq. (44) with $|r_1|$ close to 1. The system should be solved in the domain $|z| > z_c$. For nonresonant reflection, the value of $|r_1|$ in the expression for μ should be set to $\frac{U_0}{2q_F}$, and the system should be solved within the domain $1 < z < z_c$. Strictly speaking, one should multiply the transmission coefficients in both domains. Then the criterion $\frac{U_0}{2q_F}\ln(z_c) \ll 1$ ensures that the nonresonant *transmission* coefficient is close to 1. Thus, the effective transmission coefficient comes exclusively from large distances.

(vi) Our main finding is that, for weak transmission through a single Bragg mirror, the net transmission from two Bragg mirrors and the impurity can be close to 1. This enhancement of the net transmission takes place when the "Fabry-Pérot" condition $\cos\beta \approx -1$ is met. Then the denominator in Eq. (26) becomes small. This happens near certain distinct energies of the incident electron. Averaging over the phase β, employed above, requires that there are many such energies within the interval $|E_0 - E_F|$. To verify that this is the case, consider the contribution to β coming from the factor $\exp(iq_F z)$ in Eq. (33). As an estimate for z in this factor, one should take the effective length of the Bragg mirror where the reflection is formed. From Eq. (38) we see that this length is determined by the condition $y \gg 1$. At these values of y the product $y^{1/2}J_{\frac{\mu}{4q_F}+\frac{1}{2}}(y)$ saturates, meaning that the formation of the Bragg reflection is complete. The condition $y \gg 1$ transforms into the condition $z \gtrsim \frac{q_F}{E-E_F}$. Thus, the contribution to β from the accumulation of the phase Φ_{Bragg} in the course of traveling through the mirror is of the order of $(E - E_F)^{-1}$. In the relevant domain $|E_0 - E_F| \lesssim \Gamma$ this phase goes through $(2n+1)\pi$ many times. Under the experimental conditions, the averaging takes place since the energy of an incident electron is not fixed but rather distributed within a certain interval. This width of the interval can be set by finite temperature when the Friedel oscillations fall off exponentially beyond some length defined by temperature. This interval can also be set by a finite bias. Finally, if both the bias and the temperature are very low, the width of the interval can be set by finite level spacing in the wire since its length is finite.

ACKNOWLEDGMENTS

We are extremely grateful to E. G. Mishchenko for a number of illuminating discussions. The work was supported by the Department of Energy, Office of Basic Energy Sciences, Grant No. DE- FG02-06ER46313.

APPENDIX A: MAGNITUDE OF THE FRIEDEL OSCILLATIONS

The scattering of electrons from the impurity modifies the electron densities around the impurity. In the presence of electron-electron interaction this modulation of density leads to an additional scattering, which we call the "Bragg mirror" in the main text. This scattering barrier is also called the Hartree potential,

$$V_H(z) = \int_{-\infty}^{\infty} V(z-y)\delta n(y)dy, \tag{A1}$$

where $V(z-y)$ is the interaction potential and $\delta n(y)$ is the fluctuation of the density. Assuming the interaction is short ranged, $V(z-y) = \nu\,\delta(z-y)$, we see that the Hartree potential takes the form $V_H(z) = \nu\,\delta n(z)$. Now, the modulation of the electron density $\delta n(z)$, which depends on the reflection coefficient r_1, reads

$$\delta n(z) = \int_0^{q_F} \frac{dq}{\pi}\, 2\mathrm{Re}[r_1(q)\, e^{2iqz}] = \int_0^{q_F} \frac{dq}{\pi} \frac{\Gamma}{\left[\Gamma^2 + \left(q_0^2 - q^2\right)^2\right]^{1/2}} \times \cos\left(2q|z| + \tan^{-1}\frac{\Gamma}{q_0^2 - q^2}\right), \tag{A2}$$

where $q_0 = (1 + E_0)^{1/2}$ [see Eq. (7)]. Upon measuring q from q_F and introducing new variables,

$$u = 2q_0\frac{q_F - q}{\Gamma}, \quad u_0 = 2q_0\frac{q_0 - q_F}{\Gamma}, \tag{A3}$$

Eq. (A2) assumes the form

$$\delta n(z) = \frac{\Gamma}{2\pi q_0}\int_0^{\frac{2q_0q_F}{\Gamma}} du\, \frac{1}{\left[1 + (u + u_0)^2\right]^{1/2}} \times \cos\left[2|z|\left(q_F - \frac{\Gamma}{2q_0}u + \tan^{-1}\frac{1}{u + u_0}\right)\right]. \tag{A4}$$

It is convenient to separate the contributions proportional to $\sin(2q|z|)$ and to $\cos(2q|z|)$. This yields

$$\delta n(z) = \frac{\Gamma}{2\pi q_0}\int_0^{\frac{2q_0q_F}{\Gamma}} du\, \frac{1}{1 + (u + u_0)^2} \times \left\{(u + u_0)\cos\left[2|z|\left(q_F - \frac{\Gamma}{2q_0}u\right)\right] - \sin\left[2|z|\left(q_F - \frac{\Gamma}{2q_0}u\right)\right]\right\}. \tag{A5}$$

The shift $\frac{\Gamma}{2q_0}u$ of the arguments of both cosine and sine leads to the factors $\sin(\frac{\Gamma|z|}{q_0}u)$ and $\cos(\frac{\Gamma|z|}{q_0}u)$ in the numerator. For $\frac{\Gamma|z|}{q_0} \gg 1$, both terms rapidly oscillate with u. Without u dependence of the prefactor, the contribution from the cosine term will vanish. With the prefactor the contribution of this term remains much smaller than the contribution of the sine term. Retaining only the sine term, we get

$$\delta n(z) = \cos(2q_F|z|)\frac{\Gamma}{2\pi q_0}\int_0^{\frac{2q_0q_F}{\Gamma}} du\, \frac{\sin\left(\frac{\Gamma|z|}{q_0}u\right)}{1 + (u + u_0)^2}. \tag{A6}$$

For $\frac{\Gamma|z|}{q_0} \gg 1$ we can replace the upper limit of the integral by infinity and neglect the u dependence of the denominator. This leads to the final answer

$$\delta n(z) = \frac{|r_1(E_F)|^2}{2\pi|z|}\cos(2q_F|z|), \tag{A7}$$

where we have used the fact that $|r_1(E_F)|^2$ is $(1 + u_0^2)^{-1}$. Note that, unlike the conventional Friedel oscillations [19], Eq. (A7) contains the second power of $|r_1(E_F)|$. The extra power originates from the phase of the cosine in Eq. (A4), which is strongly energy dependent.

The most important outcome of the above analysis is that the Friedel oscillations are terminated at rather large distances $z = z_c \sim \frac{q_0}{\Gamma}$. We have used this value as a cutoff of log divergence in the main text.

APPENDIX B: CALCULATION OF THE TRANSMISSION COEFFICIENT FROM A MORE RIGOROUS APPROACH

Substituting the general form (39) of $a(y)$ in the system (37), we find the following general form of $b(y)$:

$$b(y) = -iy^{1/2}\left[c_1 J_{\frac{\mu}{4q_F}-\frac{1}{2}}(y) - c_2 J_{-\frac{\mu}{4q_F}+\frac{1}{2}}(y)\right]. \tag{B1}$$

Once $a(y)$ and $b(y)$ are known, the incident amplitude $A_+(y) = \frac{1}{2}[a(y) + b(y)]$ and the reflected amplitude $A_-(y) = \frac{1}{2i}[a(y) - b(y)]$ can be expressed as a combination of the Bessel functions:

$$A_+ = \frac{y^{1/2}}{2}\left\{c_1\left[J_{\frac{\mu}{4q_F}+\frac{1}{2}}(y) - iJ_{\frac{\mu}{4q_F}-\frac{1}{2}}(y)\right] + c_2\left[J_{-\frac{\mu}{4q_F}-\frac{1}{2}}(y) + iJ_{-\frac{\mu}{4q_F}+\frac{1}{2}}(y)\right]\right\}, \tag{B2}$$

$$A_- = \frac{y^{1/2}}{2i}\left\{c_1\left[J_{\frac{\mu}{4q_F}+\frac{1}{2}}(y) + iJ_{\frac{\mu}{4q_F}-\frac{1}{2}}(y)\right] + c_2\left[J_{-\frac{\mu}{4q_F}-\frac{1}{2}}(y) - iJ_{-\frac{\mu}{4q_F}+\frac{1}{2}}(y)\right]\right\}. \tag{B3}$$

In the limit $y \to \infty$, the behavior of A_+ and A_- is as follows:

$$A_+ = \frac{1}{(2\pi)^{1/2}}\left[c_2e^{i\frac{\pi\mu}{8q_F}} - ic_1e^{-i\frac{\pi\mu}{8q_F}}\right]e^{iy},$$
$$A_- = \frac{-i}{(2\pi)^{1/2}}\left[c_2e^{-i\frac{\pi\mu}{8q_F}} + ic_1e^{i\frac{\pi\mu}{8q_F}}\right]e^{-iy}. \tag{B4}$$

For small y, we have $J_{\pm\frac{\mu}{4q_F}+\frac{1}{2}}(y) \ll J_{\pm\frac{\mu}{4q_F}-\frac{1}{2}}(y)$, so the asymptotic expressions for A_+ and A_- can be written as

$$A_- = \frac{y^{1/2}}{2i}\left[ic_1J_{\frac{\mu}{4q_F}-\frac{1}{2}}(y) + c_2J_{-\frac{\mu}{4q_F}-\frac{1}{2}}(y)\right],$$
$$A_+ = \frac{y^{1/2}}{2}\left[-ic_1J_{\frac{\mu}{4q_F}-\frac{1}{2}}(y) + c_2J_{-\frac{\mu}{4q_F}-\frac{1}{2}}(y)\right]. \tag{B5}$$

To find the transmission of the Bragg mirror we need to know the ratio c_1/c_2. This ratio is determined by the condition that the Bragg mirror exists only for $y > y_c$. Correspondingly, the amplitude A_- at $y = y_c$ is zero. This yields

$$\frac{c_1}{c_2} = i\frac{J_{-\frac{\mu}{4q_F}-\frac{1}{2}}(y_c)}{J_{\frac{\mu}{4q_F}-\frac{1}{2}}(y_c)}. \tag{B6}$$

By definition, the amplitude transmission coefficient of the mirror t_{Bragg} is the ratio of the values of A_+ at $y = y_c$ and at large y. Using the ratio (B6) and Eqs. (B4) and (B5), we arrive at Eq. (40) of the main text.

APPENDIX C: ALTERNATIVE DERIVATION OF THE RESONANT REFLECTION

It is instructive to trace how the resonant reflection of $\uparrow$ electrons emerges from the closed equation for the spin component $\psi_1(z)$. To derive this equation, we introduce the

Fourier transform,

$$\varphi_2(p) = \frac{1}{2\pi}\int_{-\infty}^{\infty} dz\, \psi_2(z)\exp(-ipz), \tag{C1}$$

and we rewrite the second equation of the system (5) in the form

$$(p^2+\kappa^2)\varphi_2(p) + \frac{U_0}{2\pi}\psi_2(0) = -\frac{\alpha}{2\pi}\int_{-\infty}^{\infty} dz\, \frac{\partial\psi_1}{\partial dz}\exp(-ipz). \tag{C2}$$

Expressing $\varphi_2(p)$ and substituting it into the self-consistency condition

$$\psi_2(0) = \int_{-\infty}^{\infty} dp\, \varphi_2(p), \tag{C3}$$

we find

$$\psi_2(0) = -\frac{\alpha}{U_0+2\kappa}\int_{-\infty}^{\infty} dz\, \frac{\partial\psi_1}{\partial z}e^{-\kappa|z|}. \tag{C4}$$

Substituting Eq. (C4) into Eq. (C2), we express $\varphi_2(p)$ in terms of $\psi_1(z)$,

$$\varphi_2(p) = -\frac{\alpha}{2\pi(p^2+\kappa^2)}\left[\int_{-\infty}^{\infty} dz\frac{\partial\psi_1}{\partial z}\left(e^{-ipz} - \frac{U_0}{U_0+2\kappa}e^{-\kappa|z|}\right)\right]. \tag{C5}$$

Multiplying Eq. (C5) by $\exp(ipz)$ and integrating over p, we get the following expression for $\psi_2(z)$:

$$\psi_2(z) = \frac{\alpha}{2\kappa}\left[-\int_{-\infty}^{\infty} dz_1\frac{\partial\psi_1}{\partial z_1}e^{-\kappa|z-z_1|} + \frac{U_0e^{-\kappa|z|}}{U_0+2\kappa}\int_{-\infty}^{\infty} dz_1\frac{\partial\psi_1}{\partial z_1}e^{-\kappa|z_1|}\right], \tag{C6}$$

$$-\frac{\partial^2\psi_1}{\partial z^2} + U_0\delta(z)\psi_1 - (E+1)\psi_1 = \frac{\alpha^2}{2\kappa}\frac{\partial}{\partial z}\left[\int_{-\infty}^{\infty} dz_1\frac{\partial\psi_1}{\partial z_1}e^{-\kappa|z-z_1|} - \frac{U_0e^{-\kappa|z|}}{U_0+2\kappa}\left(\int_{-\infty}^{\infty} dz_1\frac{\partial\psi_1}{\partial z_1}e^{-\kappa|z_1|}\right)\right]. \tag{C7}$$

The term responsible for the resonant reflection is the second term on the right-hand side. Near the resonance, it is much bigger than the first term. The term $U_0\delta(z)$ on the left-hand side describes a nonresonant scattering from the impurity. Neglecting these terms, we get

$$-\frac{\partial^2\psi_1}{\partial z^2} - (E+1)\psi_1 = \frac{\alpha^2}{2}\frac{U_0}{U_0+2\kappa}\left(\int_{-\infty}^{\infty} dz_1\frac{\partial\psi_1}{\partial z_1}e^{-\kappa|z_1|}\right)e^{-\kappa|z|}\mathrm{sgn}(z). \tag{C8}$$

We see that the right-hand side is a *discontinuous* function of z. This fact constitutes the origin of the resonant reflection. For example, if we integrate Eq. (C8) near $z=0$, we will see that, unlike conventional scattering, the derivative $\frac{\partial\psi_1}{\partial z}$ is continuous at the position of the impurity. This translates into the relation $t_1 = 1 - r_1$, which is nothing but Eq. (14). To derive the second equation, Eq. (15), one should notice that $\psi_1(z)$ is present on the right-hand side only under the integral, so that the explicit solution of Eq. (C8) can be readily found. This solution also contains t_1 and r_1. Then Eq. (15) emerges as a self-consistency condition.

APPENDIX D: SMALLNESS OF THE TRANSMISSION THROUGH THE BRAGG MIRROR

The fact that the transmission coefficient $t_{\rm Bragg}$ is small suggests using the semiclassical approach to calculate $t_{\rm Bragg}$. The semiclassical approach is equivalent to the assumption that A_+ and A_-, which are the solutions of the system (34), are proportional to $\exp[\pm S(z)]$, where $S(z)$ is the action. From the system (34) we find

$$\frac{dS}{dz} = \frac{1}{2q_F}\left[\frac{\mu^2}{4z^2} - \left(E+1-q_F^2\right)^2\right]^{1/2}. \tag{D1}$$

It is seen from Eq. (D1) that the functions $A_\pm$ oscillate at $z > z_t$, where the turning point z_t is given by

$$z_t = \frac{|\mu|}{2|E+1-q_F^2|}. \tag{D2}$$

For smaller z, $A_\pm(z)$ are the combinations of growing and decaying exponents. This behavior is sustained in the interval $z_c < z < z_t$, where $z_c \sim 1/\Gamma$ is the point where the Friedel oscillations are terminated (see Appendix A). For the applicability of the semiclassics, the action

$$S(z_t) - S(z_c) = \frac{1}{2q_F}\int_{z_c}^{z_t} dz\left[\frac{\mu^2}{4z^2} - |E+1-q_F^2|^2\right]^{1/2} \tag{D3}$$

accumulated between points z_c and z_t should be much bigger than 1. However, the evaluation of the integral suggests that this condition reduces to $|\mu|/4q_F\ln(z_t/z_c) \gg 1$, which is not the case for weak electron-electron interactions. This is why we derived $t_{\rm Bragg}$ from the exact solution of the system (34). Failure of the semiclassics can be traced back to neglecting the z dependence of the prefactors A_+ and A_-.

[1] A. V. Moroz and C. H. W. Barnes, Effect of the spin-orbit interaction on the band structure and conductance of quasi-one-dimensional systems, Phys. Rev. B **60**, 14272 (1999).

[2] Y. V. Pershin, J. A. Nesteroff, and V. Privman, Effect of spin-orbit interaction and in-plane magnetic field on the conductance of a quasi-one-dimensional system, Phys. Rev. B **69**, 121306(R) (2004).

[3] D. Sánchez and L. Serra, Fano-Rashba effect in a quantum wire, Phys. Rev. B **74**, 153313 (2006).
[4] D. Sánchez, L. Serra, and M.-S. Choi, Strongly modulated transmission of a spin-split quantum wire with local Rashba interaction, Phys. Rev. B **77**, 035315 (2008).
[5] C. A. Perroni, D. Bercioux, V. M. Ramaglia, and V. Cataudella, Rashba quantum wire: Exact solution and ballistic transport, J. Phys.: Condens. Matter **19**, 186227 (2007).
[6] J. Cayao, E. Prada, P. San-Jose, and R. Aguado, SNS junctions in nanowires with spin-orbit coupling: Role of confinement and helicity on the subgap spectrum, Phys. Rev. B **91**, 024514 (2015).
[7] M. Modugno, E. Ya. Sherman, and V. V. Konotop, Macroscopic random Paschen-Back effect in ultracold atomic gases, Phys. Rev. A **95**, 063620 (2017).
[8] C. H. L. Quay, T. L. Hughes, J. A. Sulpizio, L. N. Pfeiffer, K. W. Baldwin, K. W. West, D. Goldhaber-Gordon, and R. de Picciotto, Observation of a one-dimensional spin-orbit gap in a quantum wire, Nat. Phys. **6**, 336 (2010).
[9] F. Vigneau, O. Gul, Y. M. Niquet, D. Car, S. R. Plissard, W. Escoffier, E. P. A. M. Bakkers, I. Duchemin, B. Raquet, and M. Goiran, Revealing the band structure of InSb nanowires by high-field magnetotransport in the quasiballistic regime, Phys. Rev. B **94**, 235303 (2016).
[10] J. Kammhuber, M. C. Cassidy, F. Pei, M. P. Nowak, A. Vuik, Ö. Gül, D. Car, S. R. Plissard, E. P. A. M. Bakkers, M. Wimmer, and L. P. Kouwenhoven, Conductance through a helical state in an indium antimonide nanowire, Nat. Commun. **8**, 478 (2017).
[11] T. S. Jespersen, P. Krogstrup, A. M. Lunde, R. Tanta, T. Kanne, E. Johnson, and J. Nygård, Crystal orientation dependence of the spin-orbit coupling in InAs nanowires, Phys. Rev. B **97**, 041303(R) (2018).
[12] S. Datta and B. Das, Electronic analog of the electro-optic modulator, Appl. Phys. Lett. **56**, 665 (1990).
[13] R. M. Lutchyn, J. D. Sau, and S. Das Sarma, Majorana Fermions and a Topological Phase Transition in Semiconductor-Superconductor Heterostructures, Phys. Rev. Lett. **105**, 077001 (2010).
[14] Y. Oreg, G. Refael, and F. von Oppen, Helical Liquids and Majorana Bound States in Quantum Wires, Phys. Rev. Lett. **105**, 177002 (2010).
[15] Y. J. Lin, K. Jiménez-García, and I. B. Spielman, Spinorbit-coupled Bose-Einstein condensates, Nature (London) **471**, 83 (2011).
[16] S. A. Gurvitz and Y. B. Levinson, Resonant reflection and transmission in a conducting channel with a single impurity, Phys. Rev. B **47**, 10578 (1993).
[17] J. U. Nöckel and A. D. Stone, Resonance line shapes in quasi-one-dimensional scattering, Phys. Rev. B **50**, 17415 (1994).
[18] M. P. A. Fisher and L. I. Glazman, in *Mesoscopic Electron Transport*, edited by L. Kouwenhoven, G. Schön, and L. Sohn, NATO ASI Series E (Kluwer, Dordrecht, 2013). Also available on arXiv:cond-mat/9610037.
[19] K. A. Matveev, D. Yue, and L. I. Glazman, Tunneling in One-Dimensional Non-Luttinger Electron Liquid, Phys. Rev. Lett. **71**, 3351 (1993).
[20] D. Yue, L. I. Glazman, and K. A. Matveev, Conduction of a weakly interacting one-dimensional electron gas through a single barrier, Phys. Rev. B **49**, 1966 (1994).
[21] S.-W. Tsai, D. L. Maslov, and L. I. Glazman, Phys. Rev. B **65**, 241102 (2002).
[22] A. V. Borin and K. E. Nagaev, Conductance of an interacting quasi-one-dimensional electron gas with a scatterer, Phys. Rev. B **89**, 235412 (2014).
[23] Yu. V. Nazarov and L. I. Glazman, Resonant Tunneling of Interacting Electrons in a One-Dimensional Wire, Phys. Rev. Lett. **91**, 126804 (2003).
[24] D. G. Polyakov and I. V. Gornyi, Transport of interacting electrons through a double barrier in quantum wires, Phys. Rev. B **68**, 035421 (2003).
[25] U. Fano, Effects of Configuration Interaction on Intensities and Phase Shifts, Phys. Rev. **124**, 1866 (1961).